

## Vascularized mini cooling channels to achieve temperature uniformity: Battery thermal management and electronic cooling

Turgay Coşkun, Erdal Çetkin

Online Publication Date: 05 April 2023

URL: <http://www.jresm.org/archive/resm2022.585ma1121.html>

DOI: <http://dx.doi.org/10.17515/resm2022.585ma1121>

Journal Abbreviation: *Res. Eng. Struct. Mater.*

### To cite this article

Coskun T, Çetkin E. Vascularized mini cooling channels to achieve temperature uniformity: Battery thermal management and electronic cooling. *Res. Eng. Struct. Mater.*, 2023; 9(3): 675-685.

### Disclaimer

All the opinions and statements expressed in the papers are on the responsibility of author(s) and are not to be regarded as those of the journal of Research on Engineering Structures and Materials (RESM) organization or related parties. The publishers make no warranty, explicit or implied, or make any representation with respect to the contents of any article will be complete or accurate or up to date. The accuracy of any instructions, equations, or other information should be independently verified. The publisher and related parties shall not be liable for any loss, actions, claims, proceedings, demand or costs or damages whatsoever or howsoever caused arising directly or indirectly in connection with use of the information given in the journal or related means.



Published articles are freely available to users under the terms of Creative Commons Attribution - NonCommercial 4.0 International Public License, as currently displayed at [here](https://creativecommons.org/licenses/by-nc/4.0/) (the "CC BY - NC").



Research Article

## Vascularized mini cooling channels to achieve temperature uniformity: Battery thermal management and electronic cooling

Turgay Coşkun<sup>b</sup>, Erdal Çetkin<sup>\*a</sup>

*Department of Mechanical Engineering, Izmir Institute of Technology, Izmir, Turkey*

### Article Info

#### Article history:

Received 21 Nov 2022

Revised 02 Mar 2023

Accepted 03 Apr 2023

#### Keywords:

*Silicon Heater;  
Battery Cell Mimicking  
Structures;  
Thermal Management;  
Cooling System*

### Abstract

Here we propose to use of distinct vascularized plates to be used in the applications of battery thermal management and electronic cooling. The temperatures of battery cells increase during charge and discharge; and elevated temperature values in them accelerated degradation and even may trigger battery fire because of the thermal runaway. Therefore, thermal management system is a necessity for battery packs to increase the battery performance and diminish the risk factors in the electric vehicles. Generally, high amount of heat is released in the high capacity (>15 Ah) cells in short time interval under fast charge/discharge conditions; thus, thermal management of the battery system can be achieved with liquid cooling in that situation. A silicon heater system which represents the thermal behavior of a battery cell is manufactured based on the literature and it is used in experiments. Such a method has not proposed up to now in the literature, so the study may be creating a new experimental procedure for future studies without the risk of battery fire/degradation to uncover even extreme conditions experimentally. Electronic cooling is also in prime importance due to enhanced computing requirement of current systems, and vascularized plates can solve the hot spot problems occurring with decreased energy consumption. According to the results, the cooling capacity of the vascularized plates are calculated as 20W, and a battery cell can be kept within its optimal operating temperature range when the heat loads up to 30W. Also, the temperature uniformity along the surface of mimic of the battery is satisfied by vascularized plates.

© 2023 MIM Research Group. All rights reserved.

## 1. Introduction

Recent developments in rechargeable batteries and limited energy sources of the world increase the interest of researchers on the electric vehicle industry. Vehicles are responsible for 50% of the final oil consumption in the world [1] and seen as one of the main sources of air pollution. These are key factors in the progression of electric vehicle industry. Developing electric vehicle industry bring out new issues for researchers, i.e. safety problems and performance decrements in battery cells due to overheating. Battery cell is one of the main and the most vital component in the electric vehicle. The capacity and performance of the electric vehicle mostly depend on the battery system, and it is responsible for the most of safety problems in the electric vehicle [2-4]. There are various types of battery cells and lithium-ion is one of the most commonly used types in electric vehicles. It is most popular because of high specific energy density and high specific power than others [2].

A lithium-ion battery cell consists of a negative current collector, a negative electrode, a separator, a positive electrode and a positive current collector, respectively [5, 6]. Battery cell is the basic component of the electric vehicle. A battery unit consists of many battery

\*Corresponding author: [erdalchetkin@iyte.edu.tr](mailto:erdalchetkin@iyte.edu.tr)

<sup>a</sup> orcid.org/0000-0003-3686-0208; <sup>b</sup> orcid.org/0000-0002-1921-3896

DOI: <http://dx.doi.org/10.17515/resm2022.585ma1121>

Res. Eng. Struct. Mat. Vol. 9 Iss. 3 (2023) 675-685

cells. A battery module is created by connecting many battery units in serial or parallel form and a battery pack is formed by connecting many battery modules [7]. The number of battery units in a battery pack is defined with respect to the desired voltage and capacity. The heat is generated in battery cell during charging, discharging and in operation. Therefore, the temperature of the battery cell increases. The increment in the temperature effects the capacity, performance and lifetime of the battery cell [8]. There is not uniform heat generation along the battery surface, and it is dense near the tabs. In the design of the cooling system for a battery pack, eliminating safety issues due to high temperature values (i.e. thermal runaway) and distributing heat uniformly along the battery surface and between the batteries in a battery module should be the priority. Vascularized cooling channels can be used in the cooling of the battery cells. They are commonly used in the cooling of deterministic and random heat loads [9]. Vascularized cooling channels are known for their high thermal performance and low energy consumption [10-12].

Here, a cooling system is developed for a silicon heater system which mimics the characteristics of a lithium-ion battery cell (pouch shape). A schematic view of the pouch cell is shown in Figure 1. The battery cell separated into two sections: active area and tabs. A silicon heater which is sandwiched between the steel plates was used during the experiments instead of a real battery cell. Yamada et al. [13] was used electric heater instead of real battery in the experiments. However, they were not considered the non-homogenous temperature distribution along the battery surface and heat generation rate change with charge/discharge capacity. The silicon heater reflects the thermal behavior of the battery cell and various heating loads are supplied to it in order to represent heat generation rate of a real battery under various charge/discharge rates. Using mimics of battery cells in the experimental studies eliminate some challenges associated with real battery like short-circuit, explosion, capacity fade and etc. Moreover, designed cooling system can be tested under extreme heating loads via silicon heater and will be used for electronic cooling.

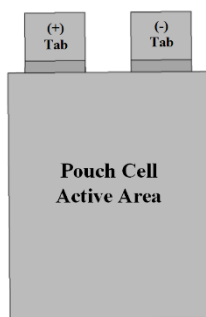


Fig. 1 A schematic of a lithium-ion pouch cell

## 2. Battery Thermal Properties

In the study, a silicon heater is used instead of real battery cell in the experiment. Therefore, the heat generation profile and thermal behavior of the battery cell need to be deeply understood to establish mimic the battery cell accurately.

### 2.1. Heat Generation in Battery Cells

The heat generation rate of the battery cell needs to be defined before introducing a cooling system for an electric vehicle. There are two main sources of generation in a battery cell. First one is the entropic heat, occurs due to the entropy change. The second one is the ohmic heat and it occurs because of the current transfer between the internal resistances

[7]. The basic equation used in the calculation of heat generation rate in a battery cell is shown in Equation 1 [14, 15].

$$q = q_{irr} + q_{rev} = I(E_{oc} - V) - \left[ IT \frac{dE_{oc}}{dT} \right] \quad (1)$$

In Equation 1,  $q$  is heat generation rate,  $I$  is current ( $I > 0$  for discharge and  $I < 0$  for charge),  $E_{oc}$  is equivalent potential (open circuit voltage),  $V$  is cell voltage,  $T$  is cell temperature and  $\frac{dE_{oc}}{dT}$  is the temperature coefficient. The first term in the Equation 1,  $I(E_{oc} - V)$ , ohmic heat generation (also called as Joule heat or irreversible heat), the second term,  $-\left[ IT \frac{dE_{oc}}{dT} \right]$ , represents the entropic heat (reversible heat) which is created by electrochemical reactions.

Heat generation at the tabs should be added to the Equation 1 to calculate total heat generation rate. The heat generation at the connection points is studied in the study of Yi et al. [16] and represented by Equation 2:

$$q_{tab} = (r + r_c)i^2 \quad (2)$$

In Equation 2,  $i$ ,  $r$  and  $r_c$  represent current density, internal resistance and contact resistance, respectively.

To sum up, the heat generation in the battery cell is shown in Equation 3 [17];

$$q_{sum} = q_{irr} + q_{rev} + q_{tab} \quad (3)$$

The total heat generation in a battery cell can be calculated by using the Equations (1), (2), (3), but, some terms in the equations are time dependent, like  $\frac{dE_{oc}}{dT}$ , so the change of these term with respect to time should be taken from experimental studies. So, if a study will be conducted without using a real battery, time dependent parameters should be defined by checking the results of experimental studies from literature or calculated using a software including battery module.

## 2.2. Parameters Effecting Heat Generation Rate in Battery Cells

Heat generation rate in a battery cell changes with respect to battery type, capacity, charge-discharge duration and ambient temperature. In addition, chemical reactions occurring inside of the battery cell also change the heat generation rate of a battery cell. The heat generation rate in a battery cell increases with enhancement in battery capacity [18]. Arora and Kapoor [18] compared heat generation rate of three different capacity cells and they figure out that heat generation rate is directly proportional to the battery capacity.

The duration of charge/discharge is symbolized by  $C$ . The charging/discharging of battery cell is completed in one hour at 1C rate. In a similar manner,  $C/2$  and  $2C$  means that charging/discharging will be completed in 2 hours and a half hour, respectively. So, charge/discharge duration is inversely related to  $C$  rate and high amount of heat releases in a short time interval at high  $C$  rates. In addition, heat generation rate in a battery cell increases logarithmically with increasing  $C$  rate [19-21].

In the study of Xie et al. [22], the heat generation rate during charging and discharging process is compared. The results of the study show that the more heat is released during discharging process when compared to charging process. The studies in the literature support the situation [17].

Ambient temperature is another parameter that has a significant effect on the heat generation rate. The effect of ambient temperature on the heat generation rate can be

explained by the change of battery internal resistances. The internal resistance of the battery is high at low temperature values. The heat generation rate is known to increase with decreasing electrical conductance at low temperature values. According to studies, the heat generation rate is inversely proportional to the ambient temperature [19, 21, 23]

The heat generation at the connections points (tabs) should be take into consideration in the calculation of total heat generation rate. The heat generation in the connection points can be observed at module and pack level in the battery systems. In the study of Keyser et al. [24], it is indicated that a cell is generated more heat when it is in a battery module rather than just a single cell. The heat generation difference between the cell in a battery module and a single cell can be reached 30% with respect to the current rate. This situation provides evidence as to how total heat generation rate is change in module or pack level.

### **2.3. Temperature Distribution on the Battery Surface**

The temperature distribution on the battery surfaces is studied detailly in the literature. The heat generation rate is denser near the tabs; therefore, the highest temperature values observed near the tabs. There are two main reasons for that situation. First one is the ionic distribution between positive and negative tabs. In the study of Li et al. [25], the effect of ionic distribution on the heat generation rate investigated numerically. Their results yield that heat generation increase with increasing ionic distribution. Second parameter is that heat generation at the tabs and it is explained in the heat generation part.

### **2.4. Battery Thermal Management**

The capacity and performance of the battery cell are changing with changing operating temperatures. There is an optimum working temperature for batteries, and it is changed with respect to battery type. Generally, lithium-ion battery cells operate best at 25-40 °C [26, 27]. The performance of the battery cell gets worse because of decrease in ion transfer at low temperatures (<15 °C). At high temperature values (>35 °C), the chemical reactions occur very fast, and it causes a decrease in the lifetime of the battery cell [28]. In addition to the operating temperatures, temperature difference along the battery surface and between the battery cells in a battery module also affect the battery performance and it causes safety problems for the electric vehicles. The temperature difference along the battery surface and between the battery cells should be kept lower than 5 °C. Because thermal runaway occurs in battery pack at high temperature values accompanying the higher temperature differences and may result in fire of the electric vehicle.

A thermal management system which satisfies the battery requirements in terms of heat generation and capacity values should be developed. In the literature, it is stated that air cooling is effective when the heat generation rate per cell is lower than 10W [29]. Therefore, liquid cooling can be sufficient in the thermal management of a high-capacity battery cell operating at high C rate.

## **3. Experimental Procedure**

A silicon heater system is used instead of real battery in the experiments. So, a silicon heater is manufactured. It is aimed to reflect battery heat generation rates and temperature distribution via the silicon heater system. So, the temperature distribution on the surface on the silicon heater is defined by benefiting from literature studies such as Wu et. al. [30], Murashko et al. [31], and Zhu et al. [32]. According to these studies, the heat generation is dense near the tabs, and it becomes less dense far away from the tabs. So, a silicon heater yielding non-homogeneous temperature distribution along the surface is manufactured. The silicon heater is sandwiched between the metal plates to have same thermal conductivity in thickness direction as it in real battery and a mimic of battery cell is created. A liquid cooling system is designed to cool the mimic of a battery cell. HEXs

having different cooling channel orientations (parallel and hybrid) are used in the cooling system. The experimental setup is shown in Figure 2. Metal plates have the thermal conductivity of 15 W/mK, which is very close to thermal conductivity of battery cell in axial directions (Figure 3). The experimental setup mainly consists of a silicon heater, a power supply, mini heat exchangers, a water bath and a data logger. There is a contact surface between the HEX and silicon heater to allow heat transfer. The remaining surfaces are insulated. The coolant liquid is supplied at the desired temperature by a water bath. The flow rate of the coolant is aligned firstly by a needle valve and then measured via a flowmeter. The temperature of the coolant liquid at the inlet and outlet of the HEX is measured via thermocouples. Also, the temperature of silicon heater is measured by thermocouples which are positioned on the surface of the silicon heater system. All the measured data are recorded via data logger.

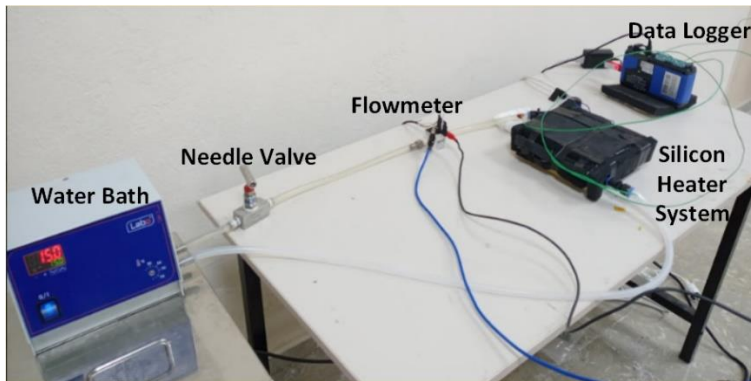


Fig. 2 Experimental setup with its components



Fig. 3 20V Silicon heater and a mimic of battery cell

#### **4. Results and Discussion**

The silicon heater system under various heating load is cooled by using different HEXs. Silicon heater voltage is 20V and maximum power extends up to 50W. The temperature and flow rate of the coolant liquid are 15 °C and 0.0218 kg/s, respectively. The power of the silicon heater is adjusted to 8W, 17W, 30W and 48W by changing the current value on the power supply. In a real battery case, heat generation rate varies under distinct C rates. In the silicon heater, heat generation in a real battery under various C rate is reflected by supplying various heating load to silicon heater. In the study, two HEXs having different heat transfer channel orientations are used: parallel and hybrid. The details of HEXs is given in Figure 4 and Table 1 [28].

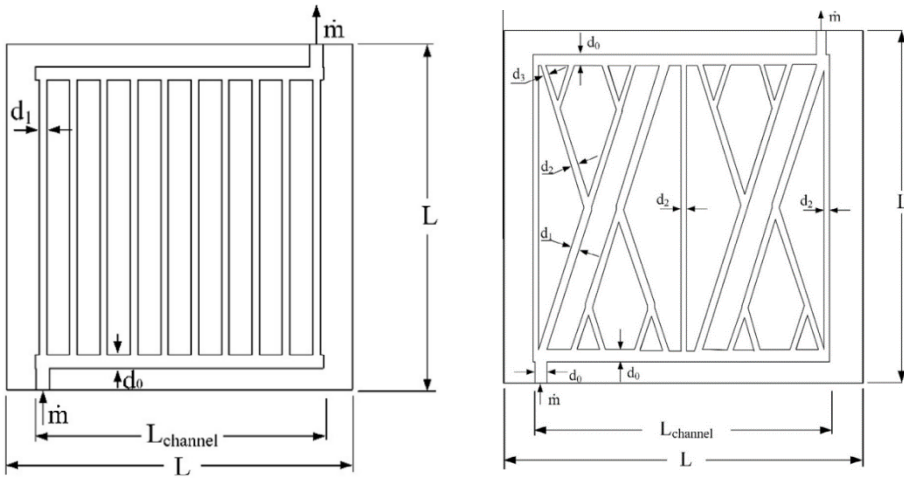


Fig. 4 Parallel and Hybrid HEXs [9]

Table 1. Dimensions of the heat exchangers [9]

#	$d_0$ (m)	$d_1$ (m)	$d_2$ (m)	$d_3$ (m)	L (m)	$L_{channel}$ (m)
Parallel Design	0.004	0.003	-	-	0.17	0.15
Hybrid Design	0.004	0.003	0.0025	0.002	0.17	0.15

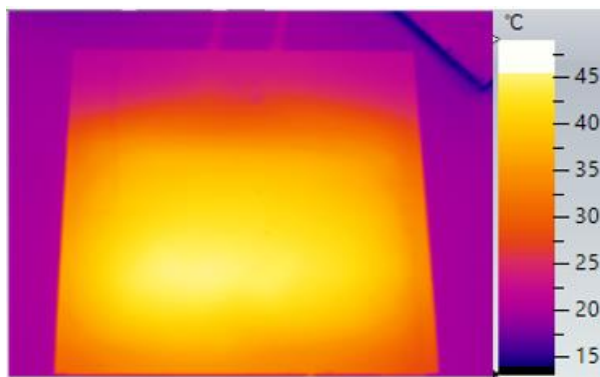


Fig. 5 Thermal image of the silicon heater surface under 30W heating load

Infrared thermal imaging of the silicon heater, when the heating load is 30W, is shown in Figure 5. According to the Figure 5, the temperature distribution is not uniform throughout the surface of the silicon heater as it in real battery case.

The silicon heater is cooled by parallel HEX and the change of temperature with respect to various heating load is shown in Figure 6. According to the Figure 6, the temperature of the silicon heater exceeds critical values when the heating load is 30W. Furthermore, the temperature of the silicon heater is kept between the operating limits when the cooling load is 17W and coolant temperature is 15°C.

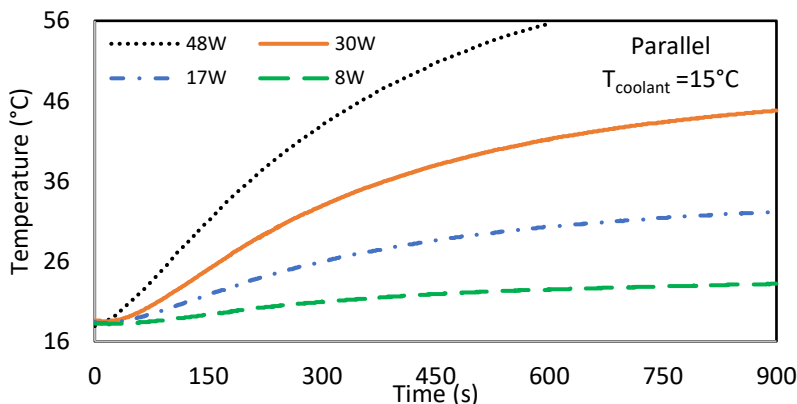


Fig. 6 The change of temperature on the surface of the silicon heater system under various heating loads (Coolant liquid: 15 °C)

The effect of cooling system on the maximum temperature values under 30W heating load when the ambient temperature is 30°C, is shown in Figure 7. The maximum temperature value reaches up to 45°C in 7.5 min when there is natural convection. In the liquid cooling, the temperature of the silicon heater reaches up to 45°C in 15 minutes when the coolant temperature is 15°C. The coolant temperature is decreased from 15°C to 10°C to keep system temperature below the critical values. According to the Figure 7, the maximum temperature values is kept below 45°C at the end of 15 minutes when the coolant temperature decreased from 15°C to 10°C.

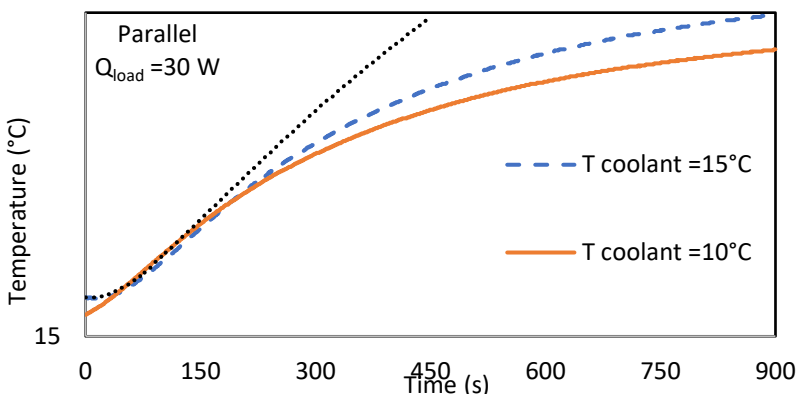


Fig. 7 The change of temperature on the surface of the silicon heater system with respect to type cooling mode and coolant temperatures (Heating load: 30 W)

In the second part of the experiment, different kinds of HEXs (parallel and hybrid) are used under various heating loads. In the following experiments, the coolant liquid temperature is fixed at 20°C. Three thermocouples are located on the surface of the silicon heater to measure temperature change during the experiments. The temperature of the silicon heater keeps below critical values for heating loads 8 W and 17 W when compared to 30W heating load, according to Figure 8 (a), (b), (c). The cooling system does not satisfy the requirements of the battery system at 30W heating load. The lowest temperature values are observed at point 3 which is very close to connection point. In addition, the temperature differences between the measurement points are lower than the 5°C.



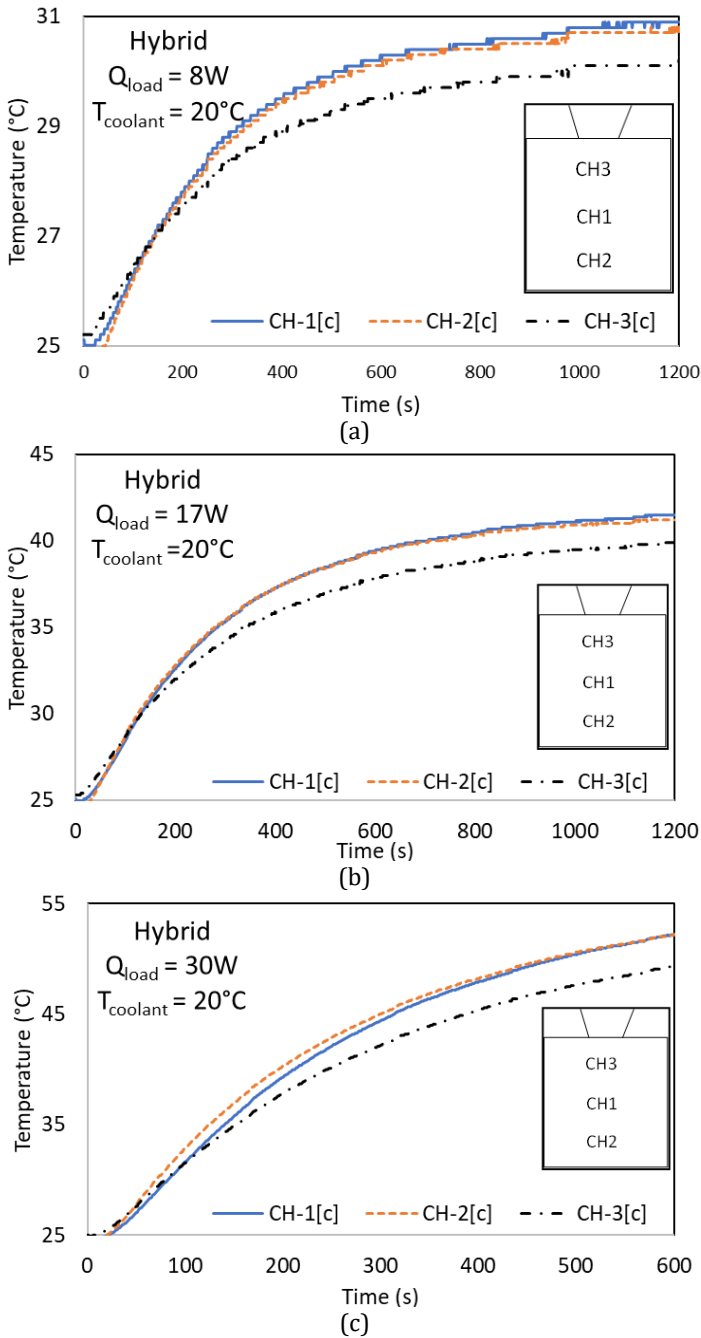


Fig. 8 The change of temperature on the surface of the silicon heater system for various heating loads: (a) 8 W, (b) 17 W and (c) 30 W

The silicon heater system cooled by parallel design HEX when the heating load is 30 W (Figure 9). Parallel design gives similar results with the hybrid design. The temperature homogeneity is satisfied by two types of HEXs ( $\Delta T < 5^{\circ}\text{C}$ ).

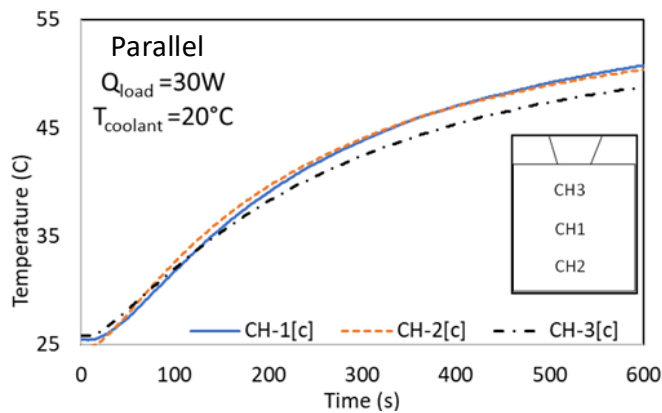


Fig. 9 The change of temperature on the surface of the silicon heater system for 30 W heating load in parallel design HEX

## 5. Conclusions

The heat generation in a battery cell is changed by many parameters such as type, capacity, charge/discharge duration and ambient temperature. The performance of the electric vehicle is highly affected by operating temperatures. So, the temperature in the battery pack should be controlled in order to improve performance and eliminate safety issues. In that study, a silicon heater system which represents the thermal behavior of a battery cell is developed to design a cooling system for a battery cell. The various heating loads (8W, 17W, 30W, 48W) are applied to the silicon heater and the cooling capacity of the vascularized cooling channels are determined. Parallel and hybrid shape cooling channels (categorized with respect to cooling channel orientations) are used in the experiments. According to the results, the temperature of the silicon heater is kept within operating limits ( $< 40^{\circ}\text{C}$ ) when the heating loads are 8W and 17W. The temperature homogeneity on the surface of silicon heater is satisfied by the cooling channels while the cooling requirements is not satisfied when the heating load is 30W. However, the temperature of the silicon heater is kept within the operating limits (under 30W heating load) at low ambient temperature ( $18^{\circ}\text{C}$ ) when the coolant liquid is  $10^{\circ}\text{C}$ . The study is an only a proximity for the cooling system of a battery cell because thermal behavior of a real battery cell under various working circumstances cannot be reflected by silicon heater system exactly. Some of the examples are chemical reactions occurring in a battery cell and the change of heat distribution on the surface of the battery cell by time. These situations are not estimated by silicon heater system. However, this method is a good approximation to design cooling system for batteries.

## Acknowledgement

The authors acknowledge that this study is supported by Izmir Institute of Technology, Scientific Research committee.

## References

- [1] IEA, 2021, Retrieved from: <https://www.iea.org/reports/key-world-energy-statistics-2021/final-consumption>.
- [2] Bandhauer TM, Garimella S, Fuller TF. A Critical Review of Thermal Issues in Lithium-Ion Batteries. Journal of the Electrochemical Society, 2011; 158: R1 - R25. <https://doi.org/10.1149/1.3515880>

- [3] Safari M, Delacourt C. Mathematical modeling of lithium iron phosphate electrode: galvanostatic charge/discharge and path dependence. *Journal of the Electrochemical Society*, 2011; 158: A63 - A73. <https://doi.org/10.1149/1.3515902>
- [4] Horie H, Abe T, Kinoshita T, Shimoida Y. A Study on an Advanced Lithium-ion Battery System for EVs. *The World Electric Vehicle Journal*, 2008; 2: 25 - 31. <https://doi.org/10.3390/wevj2020113>
- [5] Hosseinzadeh E, Marco J, Jennings P. Electrochemical-Thermal Modelling and Optimisation of Lithium-Ion Battery Design Parameters Using Analysis of Variance. *Energies*, 2017; 10: 1278(1-22). <https://doi.org/10.3390/en10091278>
- [6] Smith K, Wang CY. Power and thermal characterization of a lithium-ion battery pack for hybrid-electric vehicles. *Journal of Power Sources*, 2006; 160: 662 - 673. <https://doi.org/10.1016/j.jpowsour.2006.01.038>
- [7] Karimi G, Li X. Thermal management of lithium-ion batteries for electric vehicles. *International Journal of Energy Res.*, 2013; 37: 13 - 24. <https://doi.org/10.1002/er.1956>
- [8] Mastali M, Foreman E, Modjtahedi A, Samadani E, Amirfazli A, Farhad S, Fraser RA, Fowler M. Electrochemical-thermal modeling and experimental validation of commercial graphite/LiFePO<sub>4</sub> pouch lithium-ion batteries. *International Journal of Thermal Sciences*, 2018; 129: 218 - 230. <https://doi.org/10.1016/j.ijthermalsci.2018.03.004>
- [9] Yenigün O, Cetkin E. Experimental and numerical investigation of constructal vascular channels for self-cooling: Parallel channels, tree-shaped and hybrid designs. *International Journal of Heat and Mass Transfer*, 2016; 103: 1155 - 1165. <https://doi.org/10.1016/j.ijheatmasstransfer.2016.08.074>
- [10] Mosa M, Labat M, Lorente S. Constructal design of flow channels for radiant cooling panels, *International Journal of Thermal Sciences*, 2019; 145: 106052(1 - 14). <https://doi.org/10.1016/j.ijthermalsci.2019.106052>
- [11] Mosa M, Labat M, Lorente S. Role of flow architectures on the design of radiant cooling panels, a constructal approach, *Applied Thermal Engineering*, 2019; 150: 1345-1352. <https://doi.org/10.1016/j.applthermaleng.2018.12.107>
- [12] Sahin G, Cetkin E. Enhanced temperature uniformity with minimized pressure drops in electric vehicle battery packs at elevated C-rates. *Heat Transfer*, 2022; 51: 7540-7561. <https://doi.org/10.1002/htj.22654>
- [13] Yamada T, Koshiyama T, Yoshikawa M, Yamada T, Ono N. Analysis of a lithium-ion battery cooling system for electric vehicles using a phase-change material and heat pipes, *Journal of Thermal Science and Technology*, 2017; 12: 17-00104. <https://doi.org/10.1299/jtst.2017jtst0011>
- [14] Bernardi D, Pawlikowski E, Newman J. A general energy balance for battery systems, *Journal of the Electrochemical Society*, 1984; 132: 5 - 12. <https://doi.org/10.1149/1.2113792>
- [15] Chen Y, Evans JW. Thermal analysis of lithium polymer electrolyte batteries by a two-dimensional model-thermal behaviour and design optimization. *Electrochimica Acta*, 1994; 39: 517 - 526. [https://doi.org/10.1016/0013-4686\(94\)80095-2](https://doi.org/10.1016/0013-4686(94)80095-2)
- [16] Yi J, Kim US, Shin CB, Han T, Park S. Three-Dimensional Thermal Modeling of a Lithium-Ion Battery Considering the Combined Effects of the Electrical and Thermal Contact Resistances between Current Collecting Tab and Lead Wire. *Journal of the Electrochemical Society*, 2013; 160: A437 - A443. <https://doi.org/10.1149/2.039303jes>
- [17] Xiao M, Choe SY. Theoretical and experimental analysis of heat generations of a pouch type LiMn<sub>2</sub>O<sub>4</sub>/carbon high power Li-polymer battery. *Journal of Power Sources*, 2013; 241: 46 - 55. <https://doi.org/10.1016/j.jpowsour.2013.04.062>

- [18] Arora S, Kapoor A. Experimental Study of Heat Generation Rate during Discharge of LiFePO<sub>4</sub> Pouch Cells of Different Nominal Capacities and Thickness. *Batteries*, 2019; 5: 1 - 22. <https://doi.org/10.3390/batteries5040070>
- [19] Lin C, Xu S, Liu J. Measurement of heat generation in a 40 Ah LiFePO<sub>4</sub> prismatic battery using accelerating rate calorimetry. *International Journal of Hydrogen Energy*, 2018; 43: 8375 - 8384. <https://doi.org/10.1016/j.ijhydene.2018.03.057>
- [20] Bazinski SJ, Wang X. Predicting heat generation in a lithium-ion pouch cell through thermography and the lumped capacitance model. *Journal of Power Sources*, 2016; 305: 97 - 105. <https://doi.org/10.1016/j.jpowsour.2015.11.083>
- [21] Chen K, Unsworth G, Li X. Measurements of heat generation in prismatic Li-ion batteries. *Journal of Power Sources*, 2014; 261: 28 - 37. <https://doi.org/10.1016/j.jpowsour.2014.03.037>
- [22] Xie Y, Shi S, Tang J, Wu H, Yu J. Experimental and analytical study on heat generation characteristics of a lithium-ion power battery. *International Journal of Heat and Mass Transfer*, 2018; 122: 884 - 894. <https://doi.org/10.1016/j.ijheatmasstransfer.2018.02.038>
- [23] Arora S, Shen W, Kapoor A. Neural network based computational model for estimation of heat generation in LiFePO<sub>4</sub> pouch cells of different nominal capacities. *Computers and Chemical Engineering*, 2017; 101: 81 - 94. <https://doi.org/10.1016/j.compchemeng.2017.02.044>
- [24] Keyser M, Pesaran A, Li Q, and et al. Enabling fast charging - Battery thermal considerations, *Journal Power Sources*, 2017; 367: 228 - 236. <https://doi.org/10.1016/j.jpowsour.2017.07.00>
- [25] Li Y, Qi F, Guo H, Guo Z, Li M, Wu W. Characteristic investigation of an electrochemical-thermal coupled model for a LiFePO<sub>4</sub>/Graphene hybrid cathode lithium-ion battery, *Case Studies in Thermal Engineering*, 2019; 13: 100387(1-11). <https://doi.org/10.1016/j.csite.2018.100387>
- [26] Pesaran AA. Battery thermal models for hybrid vehicle simulations. *Journal of Power Sources*, 2002; 110: 377 - 382. [https://doi.org/10.1016/S0378-7753\(02\)00200-8](https://doi.org/10.1016/S0378-7753(02)00200-8)
- [27] Yeow K, Teng H, Thelliez M, Tan E. Thermal Analysis of a Li-ion Battery System with Indirect Liquid Cooling Using Finite Element Analysis Approach. *SAE International Journal Alt. Power*, 2012; 1: 65 - 78. <https://doi.org/10.4271/2012-01-0331>
- [28] Xu J, Lan C, Qiao Y, Ma Y. Prevent thermal runaway of lithium-ion batteries with minichannels cooling. *Applied Thermal Engineering*, 2017; 110: 883 - 890. <https://doi.org/10.1016/j.applthermaleng.2016.08.151>
- [29] Teng H, Yeow K. Design of Direct and Indirect Liquid Cooling Systems for High Capacity, High-Power Lithium-Ion Battery Packs. *SAE International Journal of Alternative Powertrains*, 2012; 1: 525 - 536. <https://doi.org/10.4271/2012-01-2017>
- [30] Wu B, Li Z, Zhang J. Thermal Design for the Pouch-Type Large-Format Lithium Ion Batteries, I. Thermo-Electrical Modeling and Origins of Temperature Non-Uniformity. *Journal of The Electrochemical Society*, 2015; 162: A181 - A191. <https://doi.org/10.1149/2.0831501jes>
- [31] Murashko K, Pyrhönen J, Laurila L. Three-Dimensional Thermal Model of a Lithium Ion Battery for Hybrid Mobile Working Machines: Determination of the Model Parameters in a Pouch Cell. *IEEE Transactions on Energy Conversion*, 2013; 28: 335 - 343. <https://doi.org/10.1109/TEC.2013.2255291>
- [32] Zhu J, Sun Z, Wie X, Dai H, Song L. Preliminary Study of a Distributed Thermal Model for a LFP Battery in COMSOL Inc. Multiphysics (MP) Software. *Vehicle Power and Propulsion Conference (VPPC)*, Beijing, China, 1-5, 2013. <https://doi.org/10.1109/VPPC.2013.6671700>